LNF-95/018

Nuclear Photofissility at Intermediate and High Energies

J.D.T. Arruda-Neto, A. Deppman, N. Bianchi, E. De Sanctis

Physical Review C, 51, 2, 751-760

Nuclear photofissility at intermediate and high energies

J.D.T. Arruda-Neto and A. Deppman
Physics Institute, University of São Paulo, P.O. Box 20516, 01452-990 São Paulo, São Paulo, Brazil

N. Bianchi and E. De Sanctis
Istituto Nazionale di Fisica Nucleare-Laboratori Nazionali di Frascati, P.O. Box 13, I-00044 Frascati, Italy

(Received 25 March 1994)

The nuclear photofissility of actinides, at intermediate and high energies, was studied by means of a formalism which makes salient the aspects of preequilibrium emissions, compound nucleus formation, and fission decay of the equilibrated system. This formalism was applied in the interpretation of the recently measured photofissilities of ^{232}Th and ^{238}U, in the energy range 300–1200 MeV, using (a) an intranuclear cascade Monte Carlo calculation to describe the preequilibrium and thermalization processes, and (b) the statistical model for the fission decay of the compound nucleus. It was found that the nonsaturation of the ^{232}Th photofissility, even at energies up to 1200 MeV, could be explained as a consequence of its higher nuclear transparency, when compared with heavier actinides. Also, the question about a possible competition between statistical and direct fission in ^{232}Th and ^{238}U was addressed.

PACS number(s): 25.85.Jg, 24.60.Dr, 27.90.+b

I. INTRODUCTION

It is a well-accepted fact that the fission of heavy nuclear systems is an excellent tool for studying the latter stages of a complex high-energy nuclear reaction [1]. A comparison of the fission predictions from a comprehensive model with experimental data can be used to test the predictions for the residue distributions from the early stage of the reactions and possibly to search for new phenomena. The use of fission as a filter for studying reactions mechanisms has been recently reviewed by Viola [2].

Projectiles with intermediate to high energies initiate an intranuclear cascade (the fast step, with a duration $\tau_0 < 10^{-22}$ s) in which particles of the continuum leave the nucleus (preequilibrium emission) all along until equilibration (compound nucleus formation); as pointed out before [3,4], in this system the thermodynamic equilibrium is reached very quickly, during a time $\tau_{eq} > (5\text{–}10)\tau_0$. In the second step (the slow step) the compound nucleus evaporates or goes into fission. There is evidence from compound nucleus studies, as well as intermediate heavy-ion reactions, that this two-step picture is valid [1].

Since fission is a slow process ($\tau_f \sim 10^{-19}$ s) that occurs from an equilibrated nuclear system, it is particularly valuable for studies of the target residues remaining after the preequilibrium emissions which, by their turn, depend on peculiar parameters as, e.g., the nuclear transparency (as addressed in the present work).

The investigation of photofission of heavy nuclei at intermediate and high energies is very convenient because (a) the primary process (photoexcitation) is well understood; (b) the photon can transfer substantial amounts of energy to the nucleus, but with relatively small transfer of linear and angular momenta, which allows the observation of excitation energy effects *alone*; and (c) as nuclear matter is very transparent to photons, the whole nuclear volume is probed in a photoexcitation process. For example, pion photoproduction would occur, in principle, with equal probability in all nucleons of the nucleus, with these nucleons acting as pion radiators.

Thus, by measuring the photofission cross section of a nucleus we can access it photofissility (the fission probability after absorption of a photon—see next section); through the study of the photofissility, important aspects of both the fission process and reaction mechanisms could be revealed.

In this paper we work out a formal approach for the analysis and interpretation of photofissility data. Through this formalism, plus the statistical model description of the fission decay, we show how novel properties of the nuclear systems could have been found out. The potentialities of this approach are demonstrated in the interpretation of recent photofissility results of ^{232}Th and ^{238}U, in the photon energy range 300–1200 MeV [5,6].

II. PHOTOFISSILITY: MAIN FEATURES

A. Definition

The photofissility $W_f(k)$ is defined as

$$W_f(k) = \frac{\sigma_f(k)}{\sigma_T(k)} , \tag{1}$$

where k is the photon energy, σ_f is the photofission cross section, and σ_T is the photoabsorption cross section (i.e., the total inelastic cross section).

Assuming that the fission decay proceeds through compound nucleus formation, we propose to write the photofission cross section related to a specific compound nucleus as

$$\sigma_f(A_{CN}, Z_{CN}; k) = \int_0^k \sigma_{CN}(A_{CN}, Z_{CN}; k) \times P_f(A_{CN}, Z_{CN}; E_x) \times N(A_{CN}, Z_{CN}; E_x, k) dE_x \ , \quad (2)$$

where $\sigma_{CN}(A_{CN}, Z_{CN}; k)$ is the cross section for the formation of the compound nucleus (A_{CN}, Z_{CN}), following absorption of a photon with energy k, P_f is its fission probability, E_x is the excitation energy, and $N(A_{CN}, Z_{CN}; E_x, k)dE_x$ is the probability of finding a compound nucleus (A_{CN}, Z_{CN}) with excitation energy between E_x and $E_x + dE_x$; we note that $0 \leq E_x \leq k$.

In the general situation, where more than one compound nucleus is formed, the experimentally observed photofission cross section is given by

$$\sigma_f(k) = \sum_{(A_{CN}, Z_{CN})} \sigma_f(A_{CN}, Z_{CN}; k) \ . \quad (3)$$

From Eqs. (1), (2), and (3), we finally get

$$W_f(k) = \frac{1}{\sigma_T(k)} \sum_{(A_{CN}, Z_{CN})} \int_0^k \sigma_{CN}(A_{CN}, Z_{CN}; k) \times P_f(A_{CN}, Z_{CN}; E_x) N(A_{CN}, Z_{CN}; E_x, k) dE_x \ . \quad (4)$$

Thus, the photofissility is a rather complete physical quantity, since it involves (a) the primary photoexcitation process (given by σ_T), (b) preequilibrium characteristics toward the formation of an equilibrated residual system (contained in both N and σ_{CN}), and (c) its fission decay probability (P_f).

The relative participation and importance of each one of these factors and the physical nature of their behavior in a wide photon energy range are addressed below.

B. Low energies: the giant resonance region

For photon energies $k \lesssim 40$ MeV, photoabsorption takes place by means of the excitation of nuclear collective modes, where the well-known giant dipole resonance dominates the whole process. In addition, preequilibrium emissions are negligible (as discussed below) and, as a consequence, the compound nucleus is the target nucleus; thus, it is quite obvious that

$$\sigma_{CN} = \sigma_T \text{ and } E_x = k \ .$$

Therefore, from Eq. (4),

$$W_f(k) = P_f(k), \text{ since } \int_0^k N(A_{CN}, Z_{CN}; E_x, k) dE_x = 1.$$

Then, the photofissility is the fission probability of the target nucleus. Because of the proximity of the fission barrier (~5–6 MeV for actinide nuclei), particularly if $k \lesssim 20$ MeV, P_f is very sensitive to the parameters of the barrier and to the neutron binding energies (since neutron evaporation is the competing decay channel). At energies near and below the barrier, $k \lesssim 8$ MeV, the fission probability reveals aspects of the multihump structure (shell effects) of the barrier and of the nuclear level densities, as well. Detailed statistical model calculations have successfully described the fission decay of actinides following photoexcitation of $E\lambda$ giant multipole resonances (GR) [7].

Thus, the investigation of photofission in the energy region of the giant resonances ($k \lesssim 40$ MeV) is restricted to the fission decay itself, since possible memory effects related to the entrance channel are unlikely. In fact, the amplitude of the GR's is not sufficiently large to drive the fission process strongly (to induce a noticeable direct fission width). The energy of motion, of the two oscillating nuclear fluids (protons and neutrons), must be damped into the compound nucleus and reappear as deformation energy before fission can take place.

C. Intermediate energies: up to m_π

Above the giant resonance region, the absorption of a photon initiates a cascade of subsequent independent collisions of the primary and secondary fast particles with the intranuclear nucleons (fast step), leading to the formation of a highly excited thermalized residual nucleus (compound nucleus). In the second (slow) step, the compound nucleus evaporates particles or undergoes fission.

The leading photoexcitation mechanism, up to the pion photoproduction threshold ($m_\pi \cong 145$ MeV), is the so-called "quasideuteron (QD) photoabsorption process." Residual nuclei are formed with excitation energies between ~ 30 and 70 MeV [8]; the fission probability of the actinide residual nuclei is nearly saturating in this energy range (see Sec. III A). Also, the QD photoabsorption cross section is a flat function of k, with comparable strengths for all heavy nuclei. Thus, one would expect to observe similar photofissilities for, e.g., all the actinides at photon energies between ~ 40 and 140 MeV; however, this is not the case, particularly for thorium and uranium—their photofissilities are very different, where the one for thorium is lower [9].

Going over our expression for W_f [Eq. (4)], it is quite intuitive to perceive that different compound nucleus characteristics would play the major role, since P_f and σ_T are comparable for all actinides. Again, we must face the problem of understanding how and why nuclei with similar masses and charges, like ^{232}Th and ^{238}U, would exhibit marked differences in their thermalization process toward compound nucleus formation.

In this regard, some tips have been provided by a recent phenomenological study of Delsanto and collaborators [10] in the QD region (~ 40–140 MeV). In their approach it is considered that the number of "active n-p pairs," contributing to the photofission process, could change from nucleus to nucleus, according to different effects of nuclear correlations on the occupation number probabilities of the nuclei energy below and above the Fermi level. These "active pairs" are those which, being excited to levels not completely occupied, contribute to transfer energy to the fission collective degrees of free-

dom, in such a way that the excited compound system undergoes fission, as stated in Ref [10]. Also, it introduced a factor (F_2, in the notation of Ref. [10]) which selects the n-p excitations useful to photofission. We show below that the introduction of this factor implies a corresponding modification in the compound nucleus cross section.

Assuming that $\sigma_T = \sigma_{\rm QD}$, where $\sigma_{\rm QD}$ is the quasideuteron photoabsorption cross section, the photofissility is expressed as (see Eq. (3) of Ref. [10])

$$W_f(k) = \frac{\sigma_f(k)}{\sigma_{\rm QD}(k)} = \frac{F_2(k)}{F_1(k)} , \qquad (5)$$

where $F_1(k) = \exp(-D/k)$ is the Pauli blocking factor.

On the other hand, we can rewrite our Eq. (4) in a simplified form, for reasoning purposes only, if we assume that the compound nuclei formed in the photofission process could be substituted by *one* mean compound nucleus $(\bar{A}_{\rm CN}, \bar{Z}_{\rm CN})$, with a mean excitation energy $\bar{E}_x$. This is quite a reasonable approximation for $k \lesssim 140$ MeV, where the $A_{\rm CN}, Z_{\rm CN}$, and E_x distribution functions are sharp and symmetric around their mean values [8]. Therefore,

$$W_f(k) \cong \frac{\sigma_{\rm CN}(\bar{A}_{\rm CN}, \bar{Z}_{\rm CN}; k)}{\sigma_{\rm QD}(k)} P_f(\bar{A}_{\rm CN}, \bar{Z}_{\rm CN}; \bar{E}_x) , \qquad (6)$$

where $\bar{E}_x = \bar{E}_x(k)$. It is obvious that if $\sigma_{\rm QD} \approx \sigma_{\rm CN}$, then $W_f \approx P_f$.

The QD cross sections scale as NZ/A, which would represent a difference of $\sim$ 2–3% between ^{238}U and ^{232}Th, while the fission probabilities of the target and residual nuclei nearly saturate for $E_x \gtrsim 50$ MeV (see, e.g., in Fig. 1 the fissility of ^{230}Th, the mean compound nucleus for $k \approx$ 100–140 MeV). Thus, comparing Eqs. (5) and (6), we conclude that

$$\sigma_{\rm CN} \cong \left(\frac{F_2}{F_1}\right) \sigma_{\rm QD} . \qquad (7)$$

The following points should be evidenced: (a) For $k = 100$ MeV, $F_2/F_1 = 1$ for ^{238}U (calculated from the expressions proposed in Ref. [10]; then, $\sigma_{\rm CN}({\rm U}) \cong \sigma_{\rm QD}$, while (b) $F_2/F_1 = 0.67$ for ^{232}Th; then, $\sigma_{\rm CN}({\rm Th}) \cong 0.67\sigma_{\rm QD}$; (c) the nonsaturation of the ^{232}Th photofissility is, thus, explained by the fact that its compound nucleus cross section is substantially lower than the photoabsorption cross section; and (d) the physical reasons for such marked difference between the thermalization processes of ^{238}U and ^{232}Th, as implied by the fact $\sigma_{\rm CN}({\rm U})/\sigma_{\rm CN}({\rm Th}) \cong 1.5$, could be tentatively found in the nucleon distribution of the fissioning nuclei and in nucleon-nucleon correlation, as addressed by Delsanto *et al.* [10]. We address this issue in Sec. IV.

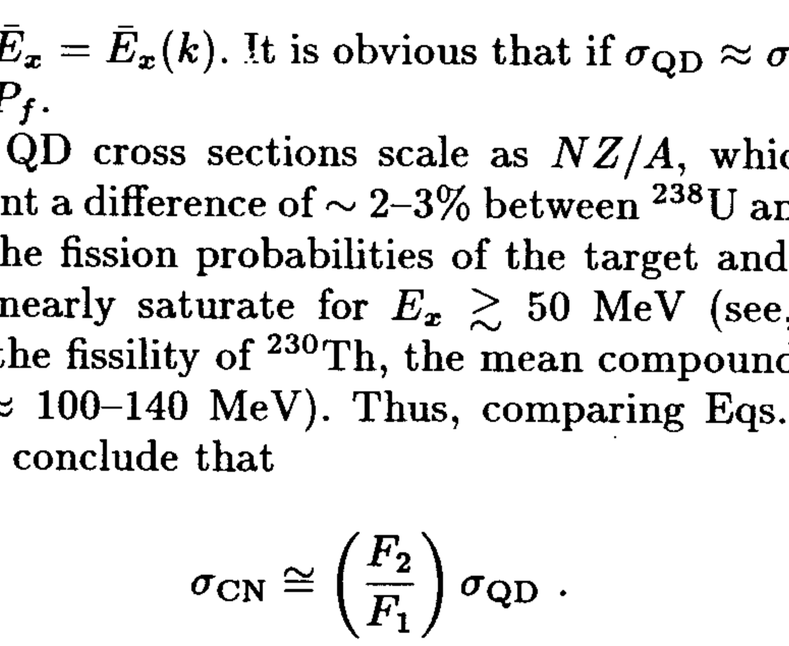

FIG. 1. Calculated fission probabilities, as a function of the excitation energy, of the most probable compound nuclei formed from the target nucleus ^{232}Th. The meaning of the dashed curves is explained in the text.

D. Intermediate to high energies: $k \gtrsim m_\pi$

Above the photopion threshold ($\sim$ 145 MeV) the nuclear photoabsorption takes place by means of two mechanisms: quasideuteron and pion production, where the latter dominates [11].

Photofission studies in this energy region were not stimulating, particularly for actinide nuclei, because of the fact that the photofissility saturates at $\sim$ 100%; even ^{232}Th was expected to saturate above a few hundreds of MeV, since its photofissility is around 60% at $k \approx 100$ MeV [9]. Therefore, with $W_f \approx 1$ no relevant information can be obtained about the fission process. Recently, this peculiarity of the actinides was explored for the delineation of the total photoabsorption cross section of uranium isotopes, from the Δ region to 1.2 GeV, by means of photofission cross sections measurements with monochromatic photons [6,12]. More recently, and quite surprisingly, however, the (γ, f) cross section of ^{232}Th, measured at Frascati in the range 250–1200 MeV [5], revealed that its photofissility remains lower than 80% even at energies as high as 1200 MeV. Since the fission probability of the most relevant compound nuclei, formed in the photoexcitation of both ^{238}U and ^{232}Th, is $\sim$ 100%, this finding for ^{232}Th cries for an explanation.

In this paper we work out a detailed study of the photofissility, where the peculiarities of the photofission process in the actinides, and ^{232}Th in particular, leading to "anomalous" W_f values, are described and interpreted on the basis of *ad hoc* model calculations.

III. PHOTOFISSILITY: MODEL CALCULATION

Given the scenario pictured for the photofissility W_f (last sections) in the wide energy range from the fission barrier to $\sim$ 1.2 GeV, plus the intriguing experimental findings for ^{232}Th, we decided to work out a calculation of W_f, using the intranuclear cascade model (INC) and a mild phenomenology, suitable for the interpretation of (γ, f) data taken for $k \gtrsim 140$ MeV. The statistical model is employed in the description of the compound nucleus fission decay.

A. Compound nucleus fission decay

The compound nucleus (CN) is the residual nucleus in which thermodynamic equilibrium has been established.

Its fission probability is defined as [13]

$$P_f(A_{\rm CN}, Z_{\rm CN}; E_x) = \sum_x P_x(A_{\rm CN}, Z_{\rm CN}; E_x) \times P_{fx}(A_{\rm CN}, Z_{\rm CN}; E_x) \ , \qquad (8)$$

where P_x is the probability that the CN, in the transition to the ground state, emits x particles, and P_{fx} is the probability that, in this case, fission occurs in one of the links of the evaporation chain. Thus,

$$P_{fx}(A_{\rm CN}, Z_{\rm CN}; E_x) = 1 - \prod_{i=1}^{x} \left[1 - \frac{\Gamma_f^{(i)}}{\sum_j \Gamma_j^{(i)}} \right] \ , \qquad (9)$$

where $\Gamma_j^{(i)}$, with $j = f, n, p, c$, are the widths for fission (f) and emission of neutrons (n), protons (p), and clusters ($c = d, \alpha$, etc.), in the i link of the evaporation chain.

For high-Z nuclei, where $\Gamma_c, \Gamma_p \ll \Gamma_f, \Gamma_n$, the evaporation of neutrons and fission are the dominant decay modes of the compound nuclei. In this case, we have that

$$P_{x(x\geq 1)}(A_{\rm CN}, Z_{\rm CN}; E_x) = \frac{\Gamma_{xn}}{\sum_j \Gamma_j^{(i)}} \ , \qquad (10)$$

where, now, x is the neutron evaporation multiplicity. P_0, the probability that the CN will not evaporate particles, is

$$P_0(A_{\rm CN}, Z_{\rm CN}; E_x) = 1 - \sum_x P_{x(x\geq 1)}(A_{\rm CN}, Z_{\rm CN}; E_x) \ . \qquad (11)$$

The partial decay width expressions for particle evaporation, $\Gamma_j (j \neq f)$, are the same given in Ref. [15], which were deduced from the statistical theory developed by Weiskopf. The fission widths Γ_f were calculated by means of well-known statistical procedures and expressions (as described in Refs. [7] and [14]), using fission barriers, neutron binding energies, and level density parameters, obtained from liquid-drop quantities calculated by the method of Myers and Swiatecki [16], and after the parametrization suggested by Guaraldo *et al.* [8] (see Ref. [8] for details). The use of liquid-drop quantities is correct, since for $E_x \gtrsim 100$ MeV shell effects are very weak, as demonstrated by Iljinov *et al.* [15]. The results for a set of the most probable compound nuclei, formed from the target nucleus ^{232}Th, is shown in Fig. 1. For all of these selected CN we found out that saturation is attained. It should be noted, however, that fission barriers, level density parameters, etc., play a crucial role in the determination of P_f magnitudes, particularly at $E_x \lesssim 100$ MeV where structure effects play some role, since the P_{fx} component of Eq. (8) involves lower and lower excitation energies as x increases. Thus, we decided to recalculate the fission probabilities, for all the most probable compound nuclei, by using as input fission barriers and level density parameters 20% higher and lower than those obtained from liquid-drop quantities (see above). The results for ^{226}Ra are shown in Fig. 1 (dashed curves). Although saturation is still attained, we note that for $E_x \lesssim 50$ MeV alterations of P_f by factors $\gtrsim 2$ are observed; these findings will be taken into account in the calculation of the fissilities (see below).

However, as E_x increases well above 50 MeV several compound nuclei, lighter than the target nucleus, can be formed. Since the fissility of each compound nucleus is, to a good extent, a function of $Z_{\rm CN}^2/A_{\rm CN}$ [17], saturation could no longer be attained, particularly when $Z_{\rm CN}$ is several unities smaller than the Z of the target nucleus. This issue is addressed in detail below.

Iljinov and Mebel [19] performed INC model calculations in the photon energy range $k \sim 60$–1200 MeV for several nuclei, obtaining $A_{\rm CN}, Z_{\rm CN}$, and E_x distributions as functions of k. The results are presented as histograms, 20 MeV wide each, of the probabilities for the following quantities: $E_x, \Delta A$, and ΔZ, where $\Delta A = A - A_{\rm CN}$ and $\Delta Z = Z - Z_{\rm CN}$; A and Z refer to the target nucleus. The mean variations $\overline{\Delta A}$ and $\overline{\Delta Z}$, and the mean excitation energy $\bar{E}_x$, are shown in Figs. 2–4, respectively. We note, from these figures, that

$$\overline{\Delta A} \cong 1.5\text{–}6 \text{ and } \overline{\Delta Z} = 0.5\text{–}2$$

in the wide k range 300–1200 MeV.

In order to fully take into account the contributions of *all* the compound nuclei formed in a process initiated by a photon of energy k, we decided to write a detailed routine for the calculation of the target nucleus fissility $P_f(A, Z; k)$. In this sense, we have that

$$P_f(A, Z; k) = \sum_{A_{\rm CN}} \sum_{Z_{\rm CN}} \sum_{E_x} P_c(A_{\rm CN}, Z_{\rm CN}; E_x, k) \times P_f(A_{\rm CN}, Z_{\rm CN}; E_x) \ , \qquad (12)$$

where $P_f(A_{\rm CN}, Z_{\rm CN}; E_x)$ was defined above [Eq. (8)], and $P_c(A_{\rm CN}, Z_{\rm CN}; E_x, k)$ is the formation probability of a compound nucleus $(A_{\rm CN}, Z_{\rm CN})$ with energy E_x, defined as

$$P_c(A_{\rm CN}, Z_{\rm CN}; E_x, k) = N_A(A_{\rm CN}; k) N_Z(Z_{\rm CN}; k) N(E_x, k). \qquad (13)$$

N_A, N_Z, and N are the probabilities for $A_{\rm CN}$, $Z_{\rm CN}$,

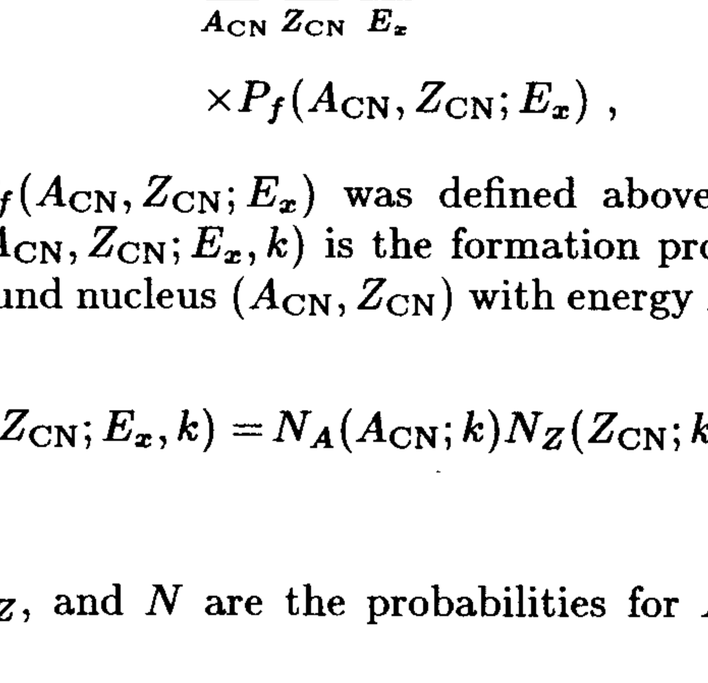

FIG. 2. Average number of nucleons emitted in the preequilibrium of ^{232}Th and ^{238}U, obtained from an INC model Monte Carlo calculation (see text).

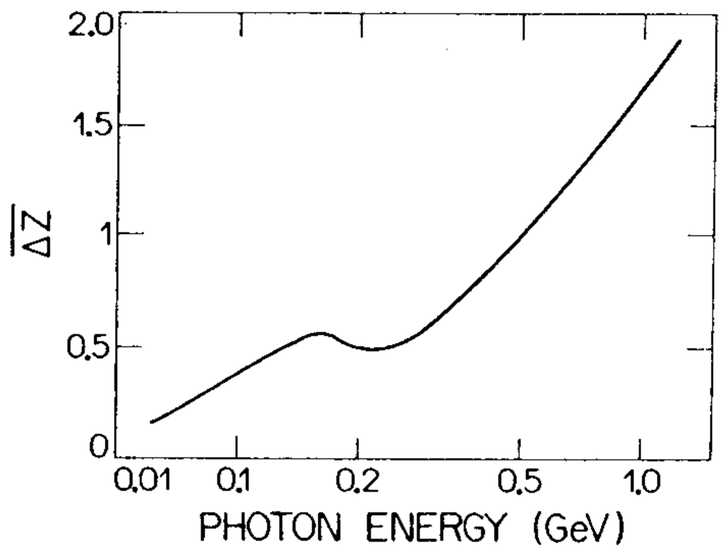

FIG. 3. Same as in Fig. 2 for the average number of protons.

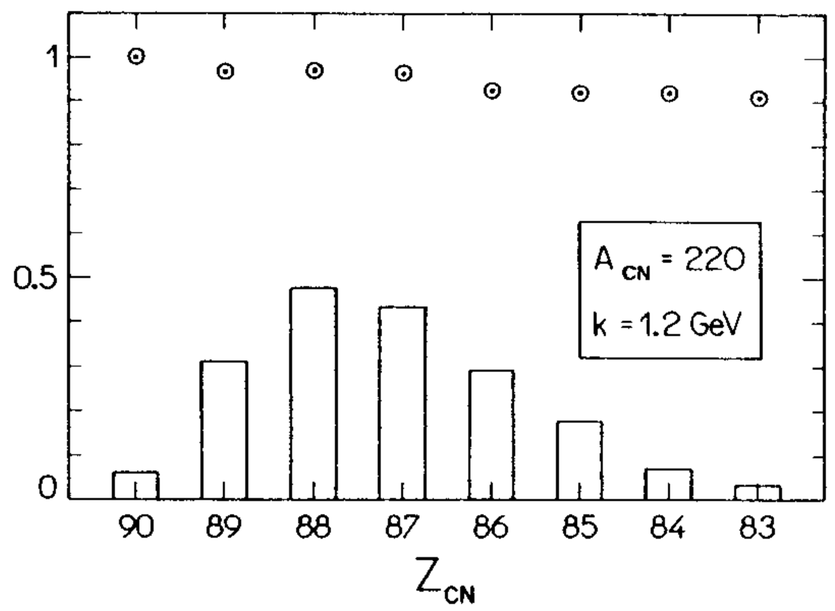

FIG. 5. Calculated E_x-averaged fissilities ($\odot$) of compound nuclei with $A_{\rm CN} = 220$ and $Z_{\rm CN}$ values ranging from 83 to 90, formed in the photoexcitation of ^{232}Th at $k = 1.2$ GeV. The heights of the histograms are proportional to the formation probabilities of the compound nuclei (see text).

and E_x, respectively, for a given k. These quantities were obtained from the INC model, Monte Carlo calculations, of Iljinov and Mebel [19].

In our routine to calculate $P_f(A, Z; k)$, Eq. (12), *all possible* compound nuclei are included, even those with very small formation probabilities. For example, at $k = 1200$ MeV, the calculations were made with $A_{\rm CN}$ and $Z_{\rm CN}$, ranging from 212 to 232, and from 81 to 90, respectively. The fission probability for each compound nucleus, $P_f(A_{\rm CN}, Z_{\rm CN}; E_x)$, was calculated in the way described above.

The main results from our calculations are the following:

(1) The fissility of both ^{232}Th and ^{238}U saturates in the whole interval $K = 300$–1200 MeV.

(2) Using Eq. (13), we can rewrite Eq. (12) in the following way,

$$P_f(A, Z; k) = \sum_{A_{\rm CN}} \sum_{Z_{\rm CN}} N_A(A_{\rm CN}; k) N_Z(Z_{\rm CN}; k) \times \left[\sum_{E_x} N(E_x, k) P_f(A_{\rm CN}, Z_{\rm CN}; E_x) \right] , \tag{12A}$$

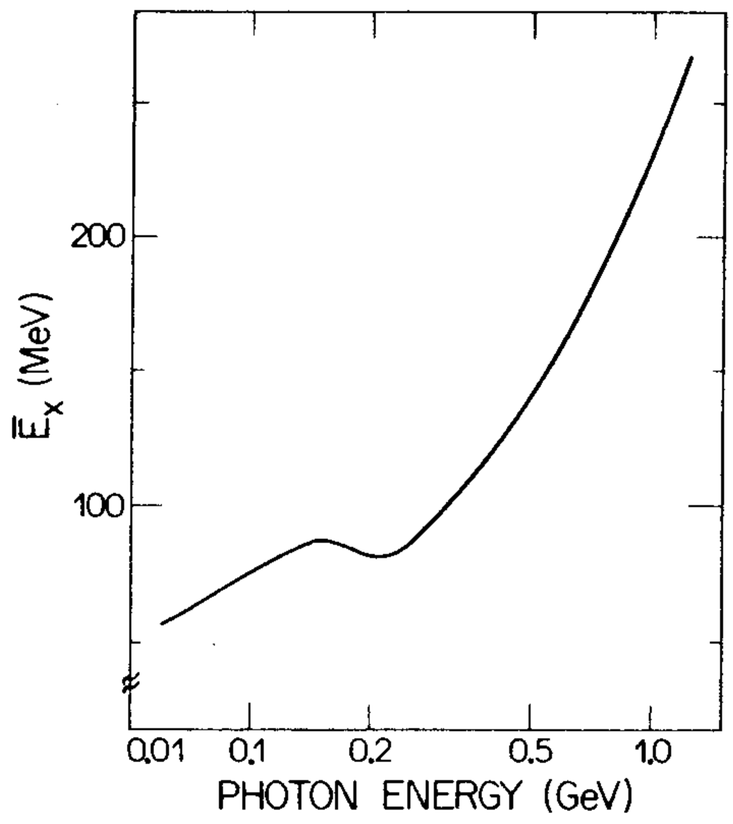

FIG. 4. Mean excitation energy $\bar{E}_x$ of ^{232}Th and ^{238}U, obtained from an INC model Monte Carlo calculation (see text).

where $\sum_{E_x} N(E_x, k) P_f(A_{\rm CN}, Z_{\rm CN}; E_x)$ is the E_x averaged CN fission probability. We show this quantity in Fig. 5, as a function of $Z_{\rm CN}$ for $A_{\rm CN} = 220$ and $k = 1200$ MeV, when ^{232}Th is the target nucleus. The heights of the histograms (Fig. 5) are proportional to $N_A N_Z$, which corresponds to the formation probabilty of a compound nucleus $(A_{\rm CN}, Z_{\rm CN})$ in the whole E_x interval: $0 - k$. It is clear from Fig. 5 that all the E_x averaged $P_f(A_{\rm CN}, Z_{\rm CN})$ are not drastically lowered for $Z_{\rm CN} < 90$, while $P_f(A_{\rm CN}, Z_{\rm CN})$ as a function of E_x is quite sensitive to changes in $Z_{\rm CN}$ for $E_x \lesssim 100$ MeV (see Fig. 1).

(3) By using $P_f(A_{\rm CN}, Z_{\rm CN}; E_x)$ values obtained with fission barriers and level density parameters lowered by 20%, the fissility of ^{232}Th decreases 5% and 3% for $k = 300$ and 1200 MeV, respectively.

(4) A "mean compound nucleus" $(\bar{A}_{\rm CN}, \bar{Z}_{\rm CN})$ can be defined, where

$$\bar{A}_{\rm CN} = A - \overline{\Delta A} \text{ and } \bar{Z}_{\rm CN} = Z - \overline{\Delta Z} \ .$$

For example, at $k = 1200$ MeV we have that (Figs. 2 and 3) $\overline{\Delta A} \cong 6$ and $\overline{\Delta Z} \cong 2$, which allow us to identify ^{226}Ra as the mean compound nucleus, when ^{232}Th is the target nucleus. We calculated the fissilities of mean compound nuclei in the interval $k = 300$–1200 MeV, for the target nuclei ^{232}Th and ^{238}U; they all saturate, too. This is somewhat expected since the fissilities of the most probable compound nuclei saturate (Fig. 1). We use this fact to simplify our theoretical approach (see below).

B. CN cross section

Assuming that $P_f(A_{\rm CN}, Z_{\rm CN}; E_x) = 1$ for $E_x \gtrsim 100$ MeV, the photofissility [Eq. (4)] can be written as

$$W_f(k) = \frac{1}{\sigma_T(k)} \sum_{(A_{\rm CN}, Z_{\rm CN})} \int_0^k \sigma_{\rm CN}(A_{\rm CN}, Z_{\rm CN}; k) \times N(A_{\rm CN}, Z_{\rm CN}; E_x, k) dE_x \ , \tag{14}$$

where

$$\int_0^k \sigma_{\rm CN}(A_{\rm CN}, Z_{\rm CN}; k) N(A_{\rm CN}, Z_{\rm CN}; E_x, k) dE_x = \sigma_{\rm CN}(A_{\rm CN}, Z_{\rm CN}; k) \ ; \quad (15)$$

then,

$$W_f(k) \cong \frac{1}{\sigma_T(k)} \sum_{(A_{\rm CN}, Z_{\rm CN})} \sigma_{\rm CN}(A_{\rm CN}, Z_{\rm CN}; k) \ . \quad (16)$$

The important qualitative message provided by Eq. (16) is that, at intermediate to high energies, the magnitude and energy dependence of the photofissility of actinide nuclei is mainly determined by the equilibration process leading to compound nucleus formation. In this sense, most of the physical information should be contained in $\sigma_{\rm CN}$, as addressed below.

The main characteristics of the compound nucleus can be derived in the framework of an intranuclear cascade (INC) model calculation [18]. The application of the (INC) model allows to take into account both the quasideuteron photoabsorption mechanism, and the single nucleon photoabsorption mechanism via one or two pion production on intranuclear nucleons. Thus, the nucleus is "heated" mainly through the scattering of the splitted nucleon pair excited in the quasideuteron process, or through absorption of the pion on a nucleon-nucleon pair.

The particles produced by the photon interaction process start an avalanche cascade of secondary particles. A fraction of these secondary particles leaves the nucleus; the remaining particles are absorbed exciting, thus, the nucleus to an energy E_x.

In this regard, we note that the INC model calculations performed by Iljinov and Mebel [19] were incorporated in our fissility calculations (see above), which helped us to demonstrate that the "mean compound nucleus approximation" is quite reasonable.

Thus, we can simplify even more our expression for W_f [Eq. (14)] if the compound nuclei involved are substituted by a "mean compound nucleus" $(\bar{A}_{\rm CN}, \bar{Z}_{\rm CN})$. With this approximation in Eq. (16) we get

$$\langle W_f(k) \rangle \cong \frac{\sigma_{\rm CN}(\bar{A}_{\rm CN}, \bar{Z}_{\rm CN}; k)}{\sigma_T(k)} \ , \quad (17)$$

where, now, $\langle W_f \rangle$ is the photofissility in the mean compound nucleus approximation.

The latter result [Eq. (17)] could be obtained intuitively, namely, since the fissility of the compound nuclei saturate (as shown above), the photofissility is a measure of the "photoexcitation efficiency" in the formation of compound nuclei. A maximum efficiency is attained only when *each* absorbed photon gives rise to a compound nucleus, that is, only when $\sigma_T = \langle \sigma_{\rm CN} \rangle$ and, therefore, $W_f = 1$ (that is, a 100% efficiency), as experimentally observed in the actinides (except for ^{232}Th).

Extending our intuitive analysis of Eq. (17), we note that when $W_f < 1$, which corresponds to $\langle \sigma_{\rm CN} \rangle < \sigma_T$, a fraction of the absorbed photons excites nonfissioning direct processes (in the fast step) and, therefore, complete thermalization is not reached. Rather intuitive, also, is the connection between this behavior and the nuclear transparency (which is related to the probability of a nucleon to escape from the nucleus without performing secondary interactions). Next we try to work out a quantitative description for these intuitive reasonings.

From the model developed by Kikuchi and Kawai [20], the CN cross section is given by

$$\sigma_{\rm CN} = \sum_{n>n_c}^{n_{\rm max}} \sigma_a^{(n)} \ , \quad (18)$$

where $\sigma_a^{(n)}$ is the partial cross section corresponding to n nucleon collisions after traversing the distance $2R$ (R is the nuclear radius), and n_c is the average number of collisions which produce nucleons with enough energy to escape from the nucleus.

Moreover,

$$\sigma_a^{(n)} = \frac{1}{2}(n+1)\pi\lambda^2 \left[1 - \sum_{i=0}^{n+1} q_i(2R/\lambda)\right] \ , \quad (19)$$

where λ is the mean free path of a nucleon in the nuclear medium, and $q_i(s/\lambda)$ is the probability that a nucleon makes i collisions after crossing a distance s; it is given by [20]

$$q_i(s/\lambda) = \frac{1}{i!}\left(\frac{s}{\lambda}\right)^i \exp\left(-\frac{s}{\lambda}\right) \ , \quad (20)$$

which, obviously, satisfies the condition

$$\sum_{i=0}^{\infty} q_i(s/\lambda) = 1 \ .$$

The projectile energy determines both the value of the parameter n_c and the number $n_{\rm max}$ of partial cross sections $\sigma_a^{(n)}$ in Eq. (18). The relevant physical quantities

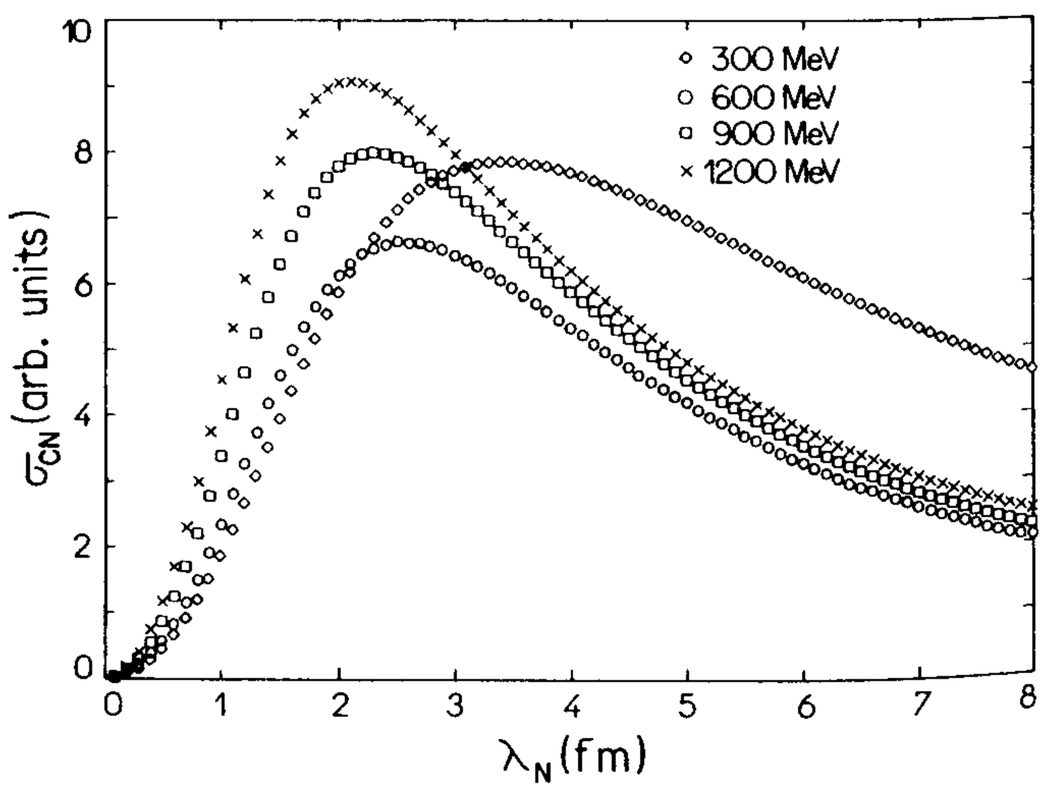

FIG. 6. Compound nucleus cross section as a function of the nucleon mean free path, calculated from a model developed by Kikuchi and Kawai [20]. The nuclear input parameters (nuclear radius, Fermi energy, Coulomb barrier, etc.) are averages of those from ^{232}Th and ^{238}U.

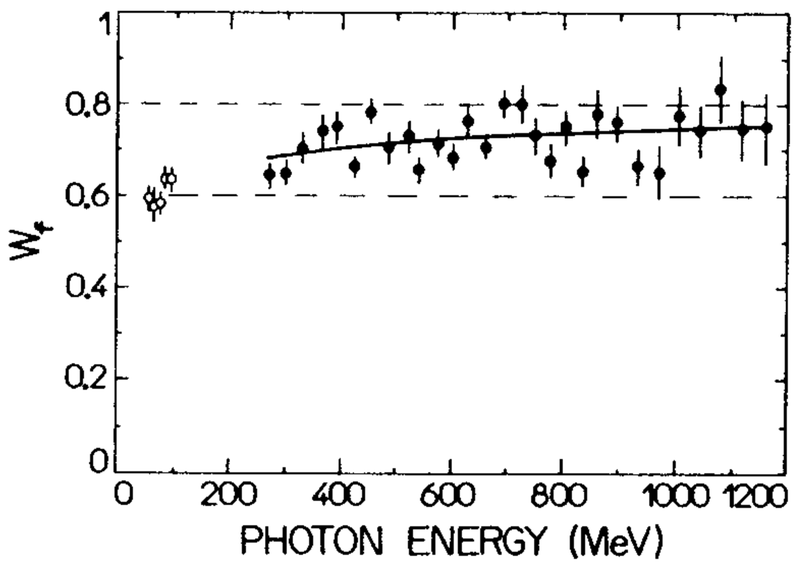

FIG. 7. Nuclear photofissility of ^{232}Th measured recently by N. Bianchi *et al.* [5] (closed circles), in the range 250–1200 MeV, and lower energy results from Ref. [9] (open circles). The solid line is a fit of the form $\ln W_f(k) = A - Bk^{-1/2}$ which ensures a visualization of the weak energy dependence of the experimental points. The horizontal dashed lines define, approximately, lower and upper limits of the data points.

related to the target nucleus are the nuclear radius [see Eq. (19)] and the Fermi energy (in the expression defining n_c); details in Ref. [20] and, in particular, in its Table 5.3.

We performed calculation of $\sigma_{\rm CN}$ as a function of λ, for the photon energies 300, 600, 900, and 1200 MeV; the results are shown in Fig. 6. It is worth to note that (1) n_c and $n_{\rm max}$ are slowly varying functions of the projectile energy; (2) the maxima of $\sigma_{\rm CN}(\lambda)$ are shifted to lower λ values when the energy increases. This aspect is particularly important for the data interpretation presented in the next section.

IV. INTERPRETATION OF W_f RESULTS FOR TH AND U

As mentioned in Sec. II D, the experimentally obtained photofissility $W_f(k)$ of ^{232}Th [5] does not saturate to 100%, even at energies as high as $k = 1.2$ GeV (Fig. 7), which is at variance with the photofissilities of heavier actinides, as ^{235}U and ^{238}U [6,12]. Taking into account the results from Leprêtre and collaborators [9], we note that the W_f of ^{232}Th exhibits a slow response, to changes of the energy, since energies as low as $k \approx 50$ MeV. A tentative description of this peculiar behavior of ^{232}Th, presented by us in a previous publication [5], using an intranuclear-evaporation Monte Carlo calculation revealed itself unsatisfactory for actinide nuclei, although reproducing well the general behavior of the fission process.

In the preceding sections we have worked out a detailed and formal description for the photofissility. It has been shown that, for energies above the giant resonances region ($k \geq 40$ MeV), the fission process no longer plays an important role (since $P_f \simeq 1$ for the compound nuclei formed after equilibration) and, as a consequence, W_f is solely determined by the mean CN cross section [Eq. (17)]. Next we try to address this problem in terms of finer nuclear properties.

We start by noting that the mean photofissility of ^{232}Th in the interval 300–1200 MeV is 0.7 (see Fig. 7), while that for ^{238}U is equal to 1 [6,12]. Since $\sigma_T({\rm U}) \cong \sigma_T({\rm Th})$, from Eq. (17) we get

$$\frac{W_f({\rm Th})}{W_f({\rm U})} \cong \frac{\langle\sigma_{\rm CN}({\rm Th})\rangle}{\langle\sigma_{\rm CN}({\rm U})\rangle} \cong 0.7 \ , \tag{21}$$

where we are using the short notation $\sigma_{\rm CN}(\bar{A}_{\rm CN}, \bar{Z}_{\rm CN}; k) \equiv \langle\sigma_{\rm CN}\rangle$.

Thus, apart from any kind of model for the compound nucleus, our approach for the photofissility enables us to conclude that certainly [Eq. (21)].

$$\langle\sigma_{\rm CN}({\rm Th})\rangle \cong 0.7\langle\sigma_{\rm CN}({\rm U})\rangle \ . \tag{22}$$

Therefore, after the absorption of a photon, ^{232}Th and ^{238}U develop quite different fast step processes toward thermalization (compound nucleus formation), in the sense that the "efficiency" of the photoexcitation in the formation of compound nuclei is higher for ^{238}U (as discussed in Sec. III B).

A. The λ interval in the photon energy range 300–1200 MeV

Recently, Tavares and Terranova [21] calculated the nuclear transparency $\tau(T_N)$ for some actinide and preactinide nuclei, as a function of the nucleon kinetic energy T_N inside the nucleus, using an expression derived by de Carvalho *et al.* [22] on the basis of the optical model, plus the "equivalent nucleus" hypothesis. Using the expression for $\tau(\lambda)$ given in Ref. [22], we converted the results of Tavares and Terranova into the form $\lambda = \lambda(T_N)$. For $T_N \gtrsim 100$ MeV the nucleon mean free path in U is nearly constant and equal to ~ 3.8 fm for neutrons, while for protons $\lambda \sim 2$–3 fm (also using the calculations of Ref. [21]).

The mean kinetic energy $\bar{T}_N$ of an emergent nucleon is given by

$$\bar{T}_N = \frac{(k - \bar{E}_x)}{\overline{\Delta A}} \ . \tag{23}$$

Using the INC-model calculations for $\bar{E}_x$ (Fig. 4) and $\overline{\Delta A}$ (Fig. 2), we estimated $\bar{T}_N$ in the photon energy range 300–1200 MeV (some figures are shown in Table I), and also the corresponding mean free paths were obtained for neutrons and protons, using $\lambda = \lambda(T_N)$ values derived from Ref. [21] (as described above).

In order to simplify our further reasonings (next paragraph), we considered an average of λ_n and λ_p as the mean free path of nucleons in general; this quantity defined as

$$\lambda_N = \frac{(A - Z)\lambda_n + Z\lambda_p}{A} \tag{24}$$

is also given in Table I. In the photon energy range 300–1200 MeV, λ_N varies between 3 and 4 fm.

In order to check our procedure we have also calculated λ_N at $k = 140$ MeV, obtaining the value $\lambda_N = 6.3$ fm,

TABLE I. Mean free paths and kinetic energies of nucleons inside ^{238}U, as a function of some photon energies. Notation defined in the text, energies are in MeV; λ's are in fm, λ_{CN} is the mean free path at the maximum of $\sigma_{CN}(\lambda)$, see Fig. 6.

k	T_N	λ_n	λ_p	λ_N	λ_{CN}
300	100	3.8	2.4	3.2	3.3
600	115	3.8	2.6	3.3	2.6
900	140	3.8	2.8	3.4	2.3
1200	160	3.8	3	3.5	2.1

which is remarkably in the middle of the λ interval 3.5–8.3 fm deduced by Leprêtre *et al.* [23], from studies of photonuclear reactions at $k < 140$ MeV in heavy nuclei.

B. λ(Th)$>$ λ(U): Another "anomaly" of thorium?

From an inspection of Table I we observe that the mean free paths of nucleons (λ_N) in ^{232}Th and ^{238}U are greater than the mean free paths (λ_{CN}) at the maxima of the calculated compound nucleus cross sections $\sigma_{CN}(\lambda)$, for $k \gtrsim 300$ MeV.

Also, from Fig. 6, $\sigma_{CN}(\lambda)$ is an approximate linear decreasing function for $\lambda \gtrsim \lambda_{CN}$. Thus, since $\sigma_{CN}(\mathrm{Th}) < \sigma_{CN}(\mathrm{U})$, we come to the conclusion that $\lambda_N(\mathrm{Th}) > \lambda_N(\mathrm{U})$, that is, in the terminology of the optical model *Th is more transparent than U*. If we assume that $\lambda_N(\mathrm{U})$=3.5 fm at k = 1200 MeV (as suggested by our calculations, Table I), and that $\sigma_{CN}(\mathrm{Th}) = 0.75\sigma_{CN}(\mathrm{U})$, we get from Fig. 6 that $\lambda_N(\mathrm{Th})$= 4.6 fm. Such difference in the nuclear transparency between two nuclear systems with comparable masses, could be explained only in terms of subtle differences in their nuclear structure. In this regard, we know from the optical model that λ_N of a particle in the nuclear matter is given by (semiclassical approximation) [24]

$$\lambda_N = \frac{E}{W_0}\sqrt{1+\frac{V_0}{E}}\frac{1}{K} , \tag{25}$$

where V_0 and W_0 are the real and imaginary parts of the optical potential, respectively, while E and K are the energy and linear momentum of the particle.

The real part of the optical potential describes the averaged nuclear potential, and is not expected to vary appreciably for the actinides. On the other hand, the imaginary part is responsible for the scattered nucleon interaction with the target nucleus intrinsic degrees of freedom, which leads to the damping of the one-particle motion. Therefore, the probability of compound nucleus formation is proportional to the imaginary part of the optical potential. This is in qualitative agreement with our conclusions extracted from a CN calculation (Fig. 6), namely, we found out that if $\sigma_{CN}(\mathrm{Th}) < \sigma_{CN}(\mathrm{U})$, as implied by our approach for the photofissility, then $\lambda_N(\mathrm{Th}) > \lambda_N(\mathrm{U})$, which is equivalent to [Eq. (25)] $W_0(\mathrm{Th}) < W_0(\mathrm{U})$. Quantitatively, however, we have that (see figures for λ_N above)

$$\frac{\lambda_N(\mathrm{U})}{\lambda_N(\mathrm{Th})} \approx \frac{W_0(\mathrm{Th})}{W_0(\mathrm{U})} \approx \frac{3.5}{4.6} \cong 0.8 .$$

We do not know what aspects of the nuclear structure, of ^{232}Th and ^{238}U, are responsible for a difference of about 20% in the imaginary parts of their optical potentials, but it is a well-known fact that ^{232}Th is an anomalous nucleus. The anomalies manifest themselves from energies as low as 4–5 MeV (triple-humped fission barrier, lower isomeric fission probability, etc., see Ref. [25] and references therein). More recently, however, Miller *et al.* [26] measured the cross sections for several ^{232}Th $(\gamma, xnyp)$ reactions at energies up to $\sim$ 140 MeV; no theoretical approach (including the hybrid model) was able to fit the higher energy region ($k \gtrsim$ 70–80 MeV) of all $(\gamma, xnyp)$ cross sections (in this energy region protons and neutrons are mostly emitted in the preequilibrium stage). Specifically, the theoretical curves drastically underestimate the experimental data, that is, the calculated preequilibrium emission cross sections are underestimated (in the evaporation region the agreement is good). It is pointed out in Ref. [26] that nothing is wrong with the hybrid model, and that maybe the problem resides in the poorly known mean free path of ^{232}Th used as one of the input parameters (other sources of uncertainties are also suggested). Since the choice of higher λ_N values generates higher preequilibrium emission rates, the experimental results for the ^{232}Th$(\gamma, xnyp)$ reactions [26] could be an additional and compelling evidence that λ_N(Th) is greater than those for heavier actinides (as suggested by our data interpretation). This is, certainly, another anomaly of ^{232}Th.

Another consequence of the fact that $W_0(\mathrm{Th}) < W_0(\mathrm{U})$ is that ^{232}Th could have, in general, more intense direct reaction components.

C. Statistical "versus" direct processes

The experimentally obtained (γ, f) cross section σ_f can be formally decomposed as

$$\sigma_f(k) = \sigma_f^{CN}(k) + \sigma_f^D(k) , \tag{26}$$

where, σ_f^{CN} is the photofission cross section via compound nucleus formation, and σ_f^D is the "direct" photofission cross section. An expression for the photofissility is obtained just by dividing Eq. (26) by $\sigma_T(k)$; then,

$$W_f(k) = W_f^{CN}(k) + W_f^D(k) . \tag{27}$$

This formal decomposition acquires a physical meaning only at high energy ($k \gtrsim$ 500 MeV) where, due to the high excitation energy ($\bar{E}_x \gtrsim$ 150 MeV), direct fission becomes a non-negligible physical possibility.

The traditional way to estimate direct components in nuclear reactions is (1) calculation of the statistical-decay component; (2) subtraction of this quantity from the experimental data; and (3) identification of this difference as the direct component. Thus, we start by deducing an analytical expression for σ_{CN}, as a function of k and $\bar{E}_x$,

TABLE II. Statistical and direct components of the photofissility. Uncertainties are $\sim 15\%$ for C and $W_f^{\rm CN}$, and $\sim 40\%$ for W_f^D.

Nucleus	k(MeV)	$W_f^{\rm exp}$	$\bar{E}_x/k$	C	$W_f^{\rm CN}$	W_f^D
^{232}Th	300	0.68	0.33	2	0.68	0
^{238}U	300	1	0.33	3	1	0
^{232}Th	600	0.72	0.28	2	0.56	0.16
^{238}U	600	1	0.28	3	0.84	0.16
^{232}Th	900	0.74	0.24	2	0.48	0.26
^{238}U	900	1	0.24	3	0.72	0.28
^{232}Th	1200	0.75	0.22	2	0.44	0.31
^{238}U	1200	1	0.22	3	0.66	0.34

in order to get $W_f^{\rm CN}$ (see below).

Kikuchi and Kawai [20] worked out a formalism to describe proton induced reactions, obtaining the following approximate expression:

$$\frac{\sigma_{\rm CN}}{\bar{E}_x} \cong \frac{\sigma_a}{(E_0+S)} \ , \tag{28}$$

where σ_a is the total absorption cross section, E_0 is the incident proton energy, and S is the separation energy (details in Ref. [20], p. 230–245). By following the same steps of the Kikuchi-Kawai formalism we found, for photonuclear reactions, that

$$\langle \sigma_{\rm CN}(\bar{E}_x) \rangle \cong C \left(\frac{\bar{E}_x}{k} \right) \sigma_T(k) \ , \tag{29}$$

where $C = C(A,Z)$ is an almost energy-independent parameter that brings the correct magnitude of $\langle \sigma_{\rm CN} \rangle$, that is, C scales the CN cross section for a given target nucleus.

Then, substituting Eq. (29) in Eq. (17), we come to

$$W_f^{\rm CN}(k) \cong C \left(\frac{\bar{E}_x}{k} \right) \ , \tag{30}$$

where the ratio $\bar{E}_x/k$ is given by the INC-model calculation (it is roughly constant for $k \gtrsim 300$ MeV, see Fig. 4). The parameter C is calculated at ~ 300 MeV, because at this lower energy $W_f^D \approx 0$ and, therefore,

$$W_f^{\rm exp}(k) \cong W_f^{\rm CN}(k) \cong C \left(\frac{\bar{E}_x}{k} \right) \ . \tag{31}$$

Finally, subtracting $W_f^{\rm CN}$ from $W_f^{\rm exp}$, we come to the direct component of the photofissility:

$$W_f^D(k) \cong W_f^{\rm exp} - C \left(\frac{\bar{E}_x}{k} \right) \ . \tag{32}$$

The results for W_f^D are shown in Table II, plus all the parameters utilized in the calculations. The $W_f^{\rm exp}$ values were taken from the solid line of Fig. 7.

Despite the large uncertainties associated to our estimation of W_f^D, it is possible to say that the "direct photofissility" of ^{232}Th is similar to that of ^{238}U. Since $W_f^{\rm CN}$ is decreasing for both ^{232}Th and ^{238}U, the slightly increasing behavior of $W_f^{\rm exp}$(Th) as a function of k is due to the onset of W_f^D(Th).

Finally, since $W_f^D({\rm Th}) \approx W_f^D({\rm U})$, it is still true that $W_f^{\rm CN}({\rm U}) > W_f^{\rm CN}({\rm Th})$, up to 1200 MeV (Table II). Thus, it remains valid the fact that $\lambda_N({\rm U}) < \lambda_N({\rm Th})$, as deduced above.

V. SUMMARY AND FINAL REMARKS

(1) We have developed a formalism for the study of the nuclear photofissility, where the following processes are clearly evidenced: (a) photoabsorption, (b) preequilibrium, CN formation, and (c) fission decay of the equilibrated system.

(2) All necessary inputs for this formalism were worked out, namely, (a) INC model Monte Carlo calculations, (b) detailed statistical calculations for the fission probabilities of the compound nuclei, and (c) estimation of the CN cross sections.

(3) This formal, computational approach was applied in the interpretation of the photofissility of ^{232}Th and ^{238}U, in the range 300–1200 MeV, highlighting (a) the close relation between photofissility and CN formation, and (b) the competition between direct and statistical fission.

(4) It was found that the surprising nonsaturation of the ^{232}Th photofissility, up to 1200 MeV, is a consequence of its higher nuclear transparency. However, given the uncertainties associated to the calculation of fission probabilities for several compound nuclei, particularly the lighter ones (as discussed in III A), we cannot completely rule out the possibility that some fraction of the $\sim 30\%$ difference, between the photofissilities of ^{232}Th and ^{238}U, is due to the fission process itself.

The computational aspects of the formalism for W_f could be both improved and extended to higher energies (up to ~ 4 GeV, as is our hope with the forthcoming photonuclear projects at CEBAF). Improvements would be welcome mostly for a better (more quantitative) calculation of $\sigma_{\rm CN}$, while the extension to higher energies implies the inclusion of cluster emission and nuclear fragmentation in the deexcitation process.

ACKNOWLEDGMENTS

We would like to thank Dr. A. S. Iljinov and Dr. M. V. Mebel for their collaboration in the early stage of this work, and by providing results of the INC calculations.

[1] Th. Blaich, M. Begemann-Blaich, M. M. Fowler, J. B. Wilhelmy, H. C. Britt, D. J. Fields, L. F. Hansen, M. N. Namboodiri, T. C. Sangster, and Z. Fraenkel, Phys. Rev. C **45**, 689 (1992), and references therein.
[2] V. E. Viola, Nucl. Phys. **A502**, 531c (1989).
[3] V. E. Bunakov, Part. Nucl. **11**, 1285 (1980).
[4] A. S. Iljinov, M. V. Mebel, C. Guaraldo, V. Lucherini, E. De Sanctis, N. Bianchi, P. Levi Sandri, V. Muccifora, E. Polli, A. R. Reolon, P. Rossi, and S. Lo Nigro, Phys. Rev. C **39**, 1420 (1989).
[5] N. Bianchi, A. Deppman, E. De Sanctis, A. Fantoni, P. Levi Sandri, V. Lucherini, V. Muccifora, E. Polli, A. R. Reolon, P. Rossi, A. S. Iljinov, M. V. Mebel, J. D. T. Arruda-Neto, M. Anghinolfi, P. Corvisiero, G. Gervino, L. Mazzaschi, V. Mokeev, G. Ricco, M. Ripani, M. Sanzone, M. Taiuti, A. Zucchiatti, R. Bergère, P. Carlos, P. Garganne, and A. Leprêtre, Phys. Rev. C **48**, 1785 (1993).
[6] N. Bianchi, A. Deppman, E. De Sanctis, A. Fantoni, P. Levi Sandri, V. Lucherini, V. Muccifora, E. Polli, A. R. Reolon, P. Rossi, M. Anghinolfi, P. Corvisiero, G. Gervino, L. Mazzaschi, V. Mokeev, G. Ricco, M. Ripani, M. Sanzone, M. Taiuti, A. Zucchiatti, R. Bergère, P. Carlos, P. Garganne, and A. Leprêtre, Phys. Lett. B **299**, 219 (1993).
[7] H. Dias, J. D. T. Arruda-Neto, B. Carlson, and M. Hussein, Phys. Rev. C **39**, 564 (1989), and references therein.
[8] C. Guaraldo, V. Lucherini, E. De Sanctis, A. S. Iljinov, M. V. Mebel, and S. Lo Nigro, Nuovo Cimento A **103**, 607 (1990).
[9] A. Leprêtre, R. Bergère, P. Bourgeois, P. Carlos, J. Fagot, J. L. Fallou, P. Garganne, A. Veyssière, H. Ries, R. Göbel, U. Kneissl, G. Mank, H. Ströher, W. Wilke, D. Ryckbosch, and J. Jury, Nucl. Phys. **A472**, 533 (1987).
[10] P. P. Delsanto, A. Fubini, F. Murgia and P. Quarati, Z. Phys. A **342**, 291 (1992).
[11] J. Ahrens, H. Gimm, R. J. Hughes, R. Leicht, P. Minn, A. Zieger, and B. Ziegler, in *Photopion Nuclear Physics*, edited by P. Stoler (Plenum, New York, 1979), p. 385.
[12] T. Frommhold, F. Steiper, W. Henkel, U. Kneissl, J. Ahrens, R. Beck, J. Peise, and M. Schmitz, Phys. Lett. B **295**, 28 (1992).
[13] A. S. Iljinov, D. I. Ivanov, M. V. Mebel, V. G. Nedorezov, A. S. Sudov, and G. Ya. Kezerashvili, Nucl. Phys. **A539**, 263 (1992).
[14] R. Vandenbosch and J. R. Huizenga, *Nuclear Fission* (Academic, New York, 1973).
[15] A. S. Iljinov, E. A. Cherepanov, and S. E. Chigrinov, Z. Phys. A **287**, 37 (1978).
[16] W. D. Myers and W. J. Swiatecki, Ark. Fyz. **36**, 343 (1967).
[17] J. B. Martins, E. L. Moreira, O. A. P. Tavares, J. L. Vieira, L. Casano, A. D'Angelo, C. Schaerf, M. L. Terranova, D. Babusci, and B. Girolami, Phys. Rev. C **44**, 354 (1991), and references therein.
[18] V. S. Barashenkov, F. G. Gereghi, A. S. Iljinov, G. G. Jonsson, and V. D. Toneev, Nucl. Phys. **A231**, 462 (1974).
[19] A. S. Iljinov and M. V. Mebel (private communication).
[20] K. Kikuchi and M. Kawai, *Nuclear Matter and Nuclear Reactions* (North Holland, Amsterdam, 1968).
[21] O. A. P. Tavares and M. L. Terranova, Z. Phys. A **343**, 407 (1992).
[22] H. G. de Carvalho, J. B. Martins, O. A. P. Tavares, R. A. M. S. Nazareth, and V. di Napoli, Nuovo Cimento **2**, 1139 (1971).
[23] A. Leprêtre, H. Beil, R. Bergère, P. Carlos, J. Fagot, and A. Veyssière, Nucl. Phys. **A390**, 240 (1982).
[24] A. G. Sitenko, *Theory of Nuclear Reactions* (World Scientific, Singapore, 1990).
[25] J. D. T. Arruda-Neto, E. Jacobs, D. De Frenne and S. Pommé, Phys. Lett. B **248**, 34 (1990), and references therein.
[26] G. J. Miller *et al.*, Nucl. Phys. **A551**, 135 (1993).